

Dwarf Novae in the OGLE Data.

II. Forty New Dwarf Novae in the OGLE-III Galactic Disk Fields*

P. Mróz¹, P. Pietrukowicz¹, R. Poleski^{1,2},
 A. Udalski¹, I. Soszyński¹, M. K. Szymański¹,
 M. Kubiak¹, G. Pietrzyński^{1,3}, Ł. Wyrzykowski^{1,4},
 K. Ulaczyk¹, S. Kozłowski¹ and J. Skowron¹

¹Warsaw University Observatory, Al. Ujazdowskie 4, 00-478 Warsaw, Poland
 e-mail: (pmroz,pietruk,rpoleski,udalski,soszynsk,msz,mk,pietrzyn,
 wyrzykow,kulaczyk,simkoz,jskowron)@astrouw.edu.pl

² Department of Astronomy, Ohio State University, 140 W. 18th Ave.,
 Columbus, OH 43210, USA

³ Universidad de Concepción, Departamento de Física, Casilla 160-C,
 Concepción, Chile

⁴ Institute of Astronomy, University of Cambridge, Madingley Road,
 Cambridge CB3 0HA, UK

ABSTRACT

We report the discovery of forty erupting cataclysmic variable stars in the OGLE-III Galactic disk fields: seventeen objects of U Gem type, four of Z Cam type, and nineteen stars showing outbursts and superoutbursts typical for SU UMa type dwarf novae. In the case of five stars we were able to estimate their supercycle lengths. The obtained lengths are in the range 20–90 d, generally between the typical SU UMa type variables and a few objects classified as the ER UMa type variables. Since there is no significant difference between the two types but a higher mass-transfer rate resulting in more frequent outbursts and superoutbursts in the ER UMa type stars, we propose to discard this type as a separate class of variables. We note that in one of the SU UMa type stars, OGLE-GD-DN-039, we found a negative supercycle period change, in contrast to other active systems of this type. Two of the new OGLE objects showed long-duration WZ Sge-like superoutbursts followed by a sequence of echo outbursts. All stars reported in this paper are part of the OGLE-III Catalog of Variable Stars.

Galaxy: disk – binaries: close – novae, cataclysmic variables

1 Introduction

Dwarf novae are eruptive cataclysmic variable (CV) stars. In these close binary systems, the magnetic field of a white dwarf is weak enough allowing the matter from a low-mass main-sequence secondary to create an accretion disk. Under certain conditions, the disk becomes unstable and the matter falls onto the surface of the white dwarf, releasing a substantial amount of gravitational energy.

The first dwarf nova (DN), U Gem, was discovered serendipitously in December 1855 by J. R. Hind during his search for minor planets (Warner 1995). By the early 1900's successive discoveries were made, *e.g.*, SS Cyg by L. Wells in 1896, Z Cam by G. Van Biesbroeck in 1904, SU UMa by L. Ceraski in 1908. In 1938 forty-seven DNe were already known (Payne-Gaposchkin & Gaposchkin 1938). The invention of photoelectric photometry in 1940s and application of CCD detectors in 1990s led to further discoveries and in-depth studies of CVs.

*Based on observations obtained with the 1.3-m Warsaw telescope at the Las Campanas Observatory of the Carnegie Institution for Science.

Gänsicke (2005) lists the most important photometric surveys, including the Palomar-Green survey (Green *et al.* 1986), the Edinburgh-Cape survey (Stobie *et al.* 1997), the Hamburg Quasar Survey (Hagen *et al.* 1995), and the 2dF Quasar Survey (Boyle *et al.* 2000), which increased the number of known CVs to several hundreds.

Recently, a large number of cataclysmic variables has been discovered mainly in the course of two projects. Based on the data from Sloan Digital Sky Survey (SDSS, York *et al.* 2000) 285 CVs were identified (Szkody *et al.* 2011), most of which had not been known before. These objects were selected using their colors and confirmed spectroscopically. Additional observations showed the presence of at least nine DN candidates in that sample (Szkody *et al.* 2011). In the second project, the Catalina Real-time Transient Survey (CRTS), numerous optical transient events, including DN outbursts, supernovae, blazars, UV Cet type flares, are being detected (Drake *et al.* 2012). So far, by June 2013, the CRTS website[†] lists around 690 confirmed and candidate CVs. From time to time new CVs and candidates for this type of variables are being detected by other optical wide-field surveys such as the Palomar Transient Factory (PTF, Law *et al.* 2009), the All Sky Automated Survey (Pojmański 1997), the OGLE Transient Survey (Kozłowski *et al.* 2013).

However, none of the mentioned above surveys concentrate on crowded stellar regions such as the Galactic disk and bulge. In the bulge area, Cieslinski *et al.* (2003) and Cieslinski *et al.* (2004) found 33 and 28 DNe, respectively, searching the OGLE-II and MACHO databases for brightenings in the light curves. Recently, Poleski *et al.* (2011) reported the identification of three new DNe detected in the OGLE-IV bulge area and presented potential of large-field high-cadence surveys for DN studies. In Fig. 1, we show the distribution of known DNe in the sky.

Based on the observed light variations DNe are divided into three main types: U Gem, SU UMa, and Z Cam variables.

U Gem type stars (also called SS Cyg type stars) exhibit quasi-regular (with recurrent times from several days to several years) large-amplitude (2–5 mag in *V*) outbursts. According to the standard model (Osaki 1974) the thermal instability in the accretion disk triggers the matter to fall onto the surface of the white dwarf. In this process a substantial amount of gravitational energy is released and the luminosity of the system increases by up to ≈ 100 times. The orbital periods of U Gem type variables are usually longer than 3 h.

SU UMa type stars have occasional superoutbursts brighter and longer than normal outbursts. During the superoutbursts light variations of an amplitude up to ≈ 0.4 mag in the *V* band, called superhumps, are observed. Currently, there are three competitive models explaining the behavior of SU UMa type variables: (1) the thermal-tidal instability (TTI) model (Osaki 1989), in which the ordinary thermal instability is coupled with the tidal instability and superhumps are the result of an eccentric disk; (2) the enhanced mass-transfer (EMT) model (Smak 1991, 2004, 2008), in which the mass-transfer rate from the secondary is variable and superhumps are due to variable brightness of the hot spot at the edge of the disk; and (3) the pure thermal limit cycle model (Cannizzo *et al.* 2010, 2012), in which the thermal instability is complex enough to produce superoutbursts and supercycles. According to the very recent work by Osaki and Kato (2013) the short cadence data from the orbiting Kepler telescope (Koch *et al.* 2010) of DNe V344 Lyr and V1504 Cyg strongly favors the TTI model. Typical SU UMa

[†]<http://nesssi.cacr.caltech.edu/catalina/AllCV.html>

type DNe have supercycle lengths P_{sc} between ≈ 100 d and ≈ 1000 d. Dwarf novae with $P_{sc} \lesssim 60$ d (so far five objects) have been classified as ER UMa type variables (Otulakowska-Hypka *et al.* 2013a), while stars with $P_{sc} \gtrsim 3000$ d are known as WZ Sge type variables (Uemura *et al.* 2010). The orbital periods of SU UMa type stars are shorter than 3 h.

Dwarf novae of the Z Cam type exhibit standstills, during which outbursts cease for days to years. In standstill the star is up to one magnitude below its outburst level. Meyer and Meyer-Hofmeister (1983) proposed that Z Cam type stars have mass-transfer rates just below the critical value in cycling outbursting phases and slightly above in standstills, as it is in the case of nova-like stars.

In this paper we report the discovery of forty DNe in the OGLE-III Galactic disk fields. Section 2 gives details on the observations and reductions. The search procedures and the analysis of light curves are described in Section 3 and Section 4, respectively. In the subsequent three sections we present the results on stars classified to the U Gem type (Section 5), SU UMa type (Section 6), and Z Cam type (Section 7). Finally, Section 8 states our conclusions.

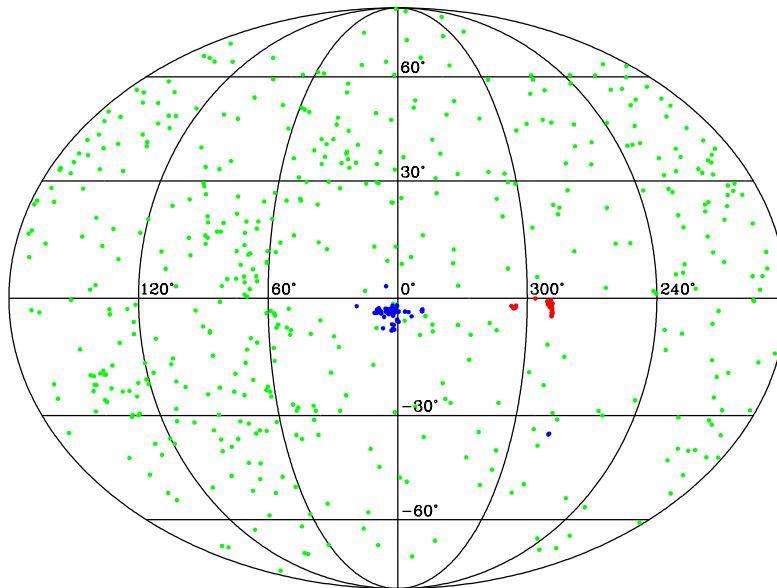


Fig. 1. Distribution, in the Galactic coordinates, of known dwarf novae. Green points denote positions of 507 DNe listed in the 2013 version of the Ritter & Kolb catalog (Ritter & Kolb 2003), blue points represent 65 DNe found in the OGLE-II and MACHO Galactic bulge data (Cieslinski *et al.* 2003 and Cieslinski *et al.* 2004, respectively), while red points show positions of 40 new DNe reported in this paper.

2 Observations and Data Reductions

All data presented in this paper were collected between 2001 and 2009 during the third phase of the Optical Gravitational Lensing Experiment (OGLE-III). The observations were obtained with the 1.3-m Warsaw Telescope located at Las Campanas Observatory, Chile, which is operated by Carnegie Institution

for Science. A CCD camera attached to the telescope consisted of eight chips with the total field of view of $35' \times 35'$ and the scale of 0.26 arcsec/pixel. More details concerning the instrumentation can be found in Udalski (2003).

The OGLE-III Galactic disk fields cover an area of 7.12 deg² toward the constellations of Carina, Centaurus, and Musca. The time-span of the observations and the number of data points varied from field to field (see Table 1 and Figs. 1–2 in Pietrukowicz *et al.* 2013). A total number of approximately $8.8 \cdot 10^6$ stars was observed (Szymański *et al.* 2010) in these lines-of-site.

A majority of observations were taken in the standard *I*-band filter with an exposure time of 120 or 180 s. For the remaining measurements, the *V*-band filter was used with a longer exposure time of 240 s. The photometry was carried out with the Difference Image Analysis (DIA) algorithm (Alard and Lupton 1998, Woźniak 2000). A detailed description of the OGLE data reduction pipeline can be found in Udalski *et al.* (2008).

In the case of eighteen faint DNe, we decided to improve their photometry. For this purpose we selected subtracted images taken during outbursts of the DNe under good seeing conditions. After stacking the images, we re-determined positions of the centroids for these stars. Finally, having the new centroids, we extracted the photometry using the standard pipeline.

The final *I*-band light curves of the newly detected dwarf novae are available to the astronomical community from the OGLE Internet Archive:

<http://ogle.astroww.edu.pl>
<ftp://ftp.astroww.edu.pl/ogle/ogle3/OIII-CVS/gd/dn/>

The objects are arranged according to increasing right ascension and named as OGLE-GD-DN-NNN, where NNN is a consecutive number. We note that DNe reported in this paper are included in the OGLE-III Catalog of Variable Stars.

3 Search for Dwarf Novae

Dwarf novae exhibit a vast diversity of photometric behavior. Their light curve shapes often differ much even for members of the same subgroup. Outbursts appear unexpectedly, and in many cases, they recur non-periodically. All these factors make the search for dwarf novae very demanding. Our search procedure consisted of three independent parts.

In the beginning, 27 DNe were discovered as a byproduct of the search for periodic variable stars in the OGLE-III Galactic disk fields (Pietrukowicz *et al.* 2013). Phased and time-domain light curves of almost 345 500 stars with a signal to noise $S/N > 10$ were visually inspected resulting in thousands of periodic variables such as eclipsing binaries (Pietrukowicz *et al.* 2013), pulsating stars, and spotted stars (Pietrukowicz *et al.* in preparation). We identified the first 27 DNe, mainly with large amplitudes and quasi-periodic brightenings, among miscellaneous variables. This relatively large number of DNe encouraged us to further investigations.

It is commonly known that the majority of cataclysmic variables and particularly dwarf novae exhibit UV and blue excess (Warner 1995). Unfortunately, the observations were collected only in the optical *V*- and *I*-bands. Due to large interstellar absorption in the observed disk fields, this makes a color-based selection of CVs/DNe practically impossible. On the other hand, we decided to examine the optical counterparts to the X-ray sources detected within the OGLE-III disk area (Balman 2012, Udalski *et al.* 2012). According to the

HEASARC (the High Energy Astrophysics Science Archive Research Center[‡]) database there are 220 such sources. We searched for optically variable candidates within the radius of $5''.2$ ($=20$ pix) around their positions. Only one dwarf nova, OGLE-GD-DN-030, was found $0''.47$ away from the source X110505.31-611044.5 (Ptak & Griffiths 2003). Incidentally, we note that this source is located $3''.8$ away from the pulsar PSR J1105-6107, which was observed with the Chandra X-Ray Observatory twice in 2002. This result shows that the current X-ray surveys are shallow and/or limited to small regions in the sky.

We were aware that some DNe might have been overlooked during the visual inspection or they simply did not pass the periodicity condition (*e.g.*, only one outburst was observed). In order to increase the completeness as much as possible, we applied the following procedure. For all $\approx 8.8 \cdot 10^6$ stars with the available *I*-band photometry observations were grouped into one-day bins and the mean brightness per night with at least three data points was calculated. In the first approach, DN candidates were selected if their brightness increased by at least 1.0 mag over the mean value for at least three consecutive days. From about 12 500 visually inspected candidates we found twelve new dwarf novae. In the second approach, we extended the search for variables with amplitudes at least 0.8 mag and a mean brightness $I < 19.5$ mag, but no new objects were found. Our algorithm found 24 DNe already detected in the first part. It did not recognize two Z Cam type stars and two SU UMa type variables with amplitudes between 0.3 and 0.8 mag, which are very likely blended objects. Apart from the *bona fide* DNe, the majority of candidates were DY Per type stars, Be stars, long period variables, and artifacts.

The three independent searches resulted in the discovery of 40 previously unknown DNe. None of them is listed neither in the Ritter & Kolb catalog (Ritter & Kolb 2003, RKcat Edition 7.19, 2013) nor in the General Catalogue of Variable Stars, (GCVS, Samus *et al.*, 2007–2012). In Table 1, we give basic information on the discovered DNe. Figs. 2–3 present finding charts for our objects.

4 Light Curve Analysis

We cleaned the raw light curves of our DNe removing a few obvious outliers and all data points fainter than $I = 23$ mag. Observations were calibrated on the basis of the mean magnitudes given in the OGLE-III photometric maps of the Galactic disk (Szymański *et al.* 2010). Each final light curve contains from 678 (OGLE-GD-DN-001) to 3789 (OGLE-GD-DN-009) data points with the mean value of 1752 points. The time span of the observations varies from 1 to 7 years, depending on the field.

Each light curve was divided into parts corresponding to quiescence, outbursts, superoutbursts, and standstills, if those were present. The magnitudes were transformed into flux and the weighted mean was calculated for quiescence and standstills. We note that the statistical error is small (typically $\sigma_I \lesssim 0.05$ mag) due to the large number of measurements. In a similar way, the peak brightness was assessed for normal outbursts and superoutbursts of SU UMa type variables. We measured the time duration of the outbursts and calculated their average value. In many cases the beginning or/and the end of outburst was not observed. For some SU UMa type stars we were able to find the recurrence times of normal outbursts (T_n) and superoutbursts (T_s). In a

[‡]<http://heasarc.gsfc.nasa.gov/>

Table 1: Basic data on the discovered DNe in the OGLE-III disk fields

Name	Field	Star ID	RA J2000.0	Dec J2000.0	Type
OGLE-GD-DN-001	CAR118.8	1241	10 ^h 36 ^m 19 ^s .78	-63°37'32".8	SU/WZ
OGLE-GD-DN-002	CAR116.2	10591	10 ^h 37 ^m 28 ^s .40	-62°49'28".8	UG
OGLE-GD-DN-003	CAR118.7	29174	10 ^h 38 ^m 00 ^s .57	-63°22'47".7	SU
OGLE-GD-DN-004	CAR116.3	27971	10 ^h 38 ^m 45 ^s .69	-62°38'52".0	SU
OGLE-GD-DN-005	CAR116.3	6361	10 ^h 38 ^m 56 ^s .17	-62°43'15".8	UG
OGLE-GD-DN-006	CAR117.8	28538	10 ^h 39 ^m 47 ^s .75	-62°55'29".4	UG
OGLE-GD-DN-007	CAR117.7	31482	10 ^h 39 ^m 57 ^s .00	-62°45'17".8	SU
OGLE-GD-DN-008	CAR117.5	13030	10 ^h 40 ^m 14 ^s .25	-62°33'17".7	SU
OGLE-GD-DN-009	CAR109.7	35705	10 ^h 42 ^m 02 ^s .40	-62°11'53".5	SU
OGLE-GD-DN-010	CAR110.1	28587	10 ^h 43 ^m 30 ^s .62	-61°47'36".8	UG
OGLE-GD-DN-011	CAR109.3	16569	10 ^h 43 ^m 34 ^s .50	-62°07'34".4	UG
OGLE-GD-DN-012	CAR107.5	5148	10 ^h 46 ^m 16 ^s .97	-61°50'56".8	ZC
OGLE-GD-DN-013	CAR111.3	38101	10 ^h 47 ^m 46 ^s .92	-60°41'08".8	UG
OGLE-GD-DN-014	CAR111.3	39243	10 ^h 47 ^m 57 ^s .16	-60°41'22".7	SU/WZ
OGLE-GD-DN-015	CAR108.1	17123	10 ^h 47 ^m 58 ^s .43	-61°38'17".7	SU
OGLE-GD-DN-016	CAR108.2	16574	10 ^h 48 ^m 07 ^s .40	-61°30'13".5	SU
OGLE-GD-DN-017	CAR105.8	42407	10 ^h 50 ^m 16 ^s .68	-61°50'09".1	SU
OGLE-GD-DN-018	CAR105.8	44632	10 ^h 50 ^m 47 ^s .10	-61°50'09".7	UG
OGLE-GD-DN-019	CAR105.5	24506	10 ^h 51 ^m 36 ^s .65	-61°27'39".1	UG
OGLE-GD-DN-020	CAR105.7	51393	10 ^h 52 ^m 11 ^s .85	-61°41'14".3	UG
OGLE-GD-DN-021	CAR105.3	33886	10 ^h 52 ^m 49 ^s .48	-61°34'16".5	UG
OGLE-GD-DN-022	CAR105.4	38638	10 ^h 54 ^m 00 ^s .44	-61°24'38".3	UG
OGLE-GD-DN-023	CAR104.7	1357	10 ^h 55 ^m 03 ^s .97	-61°56'52".8	SU
OGLE-GD-DN-024	CAR114.5	2145	10 ^h 55 ^m 20 ^s .52	-60°17'28".1	UG
OGLE-GD-DN-025	CAR113.6	11221	10 ^h 57 ^m 17 ^s .30	-61°02'04".4	SU
OGLE-GD-DN-026	CAR104.7	60634	10 ^h 57 ^m 30 ^s .00	-61°40'30".3	UG
OGLE-GD-DN-027	CAR114.1	36099	10 ^h 57 ^m 50 ^s .90	-60°37'22".6	ZC
OGLE-GD-DN-028	CAR113.1	31667	10 ^h 59 ^m 25 ^s .08	-61°17'27".1	ZC
OGLE-GD-DN-029	CAR106.6	38520	11 ^h 02 ^m 35 ^s .82	-61°44'09".4	UG
OGLE-GD-DN-030	CAR100.7	27497	11 ^h 05 ^m 05 ^s .36	-61°10'44".8	UG
OGLE-GD-DN-031	CAR100.2	37818	11 ^h 07 ^m 20 ^s .59	-61°08'32".9	SU
OGLE-GD-DN-032	CEN107.8	52448	11 ^h 53 ^m 56 ^s .20	-62°12'10".6	UG
OGLE-GD-DN-033	MUS100.5	4312	13 ^h 12 ^m 50 ^s .74	-64°39'51".2	SU
OGLE-GD-DN-034	MUS100.6	5148	13 ^h 12 ^m 53 ^s .85	-64°49'55".6	SU
OGLE-GD-DN-035	MUS100.1	65558	13 ^h 15 ^m 08 ^s .56	-65°00'23".8	ZC
OGLE-GD-DN-036	MUS100.1	25683	13 ^h 15 ^m 29 ^s .03	-65°05'38".0	SU
OGLE-GD-DN-037	MUS101.8	64830	13 ^h 22 ^m 16 ^s .09	-65°08'00".5	SU
OGLE-GD-DN-038	MUS101.7	38066	13 ^h 23 ^m 57 ^s .46	-65°04'35".7	SU
OGLE-GD-DN-039	MUS101.8	33967	13 ^h 24 ^m 01 ^s .62	-65°12'19".8	SU
OGLE-GD-DN-040	CEN108.8	42697	13 ^h 32 ^m 39 ^s .50	-64°28'35".9	UG

Object OGLE-GD-DN-009 also refers to star 28443 in field CAR115.2.

few cases the superoutbursts were well-sampled and bright enough that it was possible to determine the superhump period after linear de-trending. For three U Gem type stars we were able to estimate their orbital periods in quiescence. This was performed with the help of the TATRY code (Schwarzenberg-Czerny 1996).

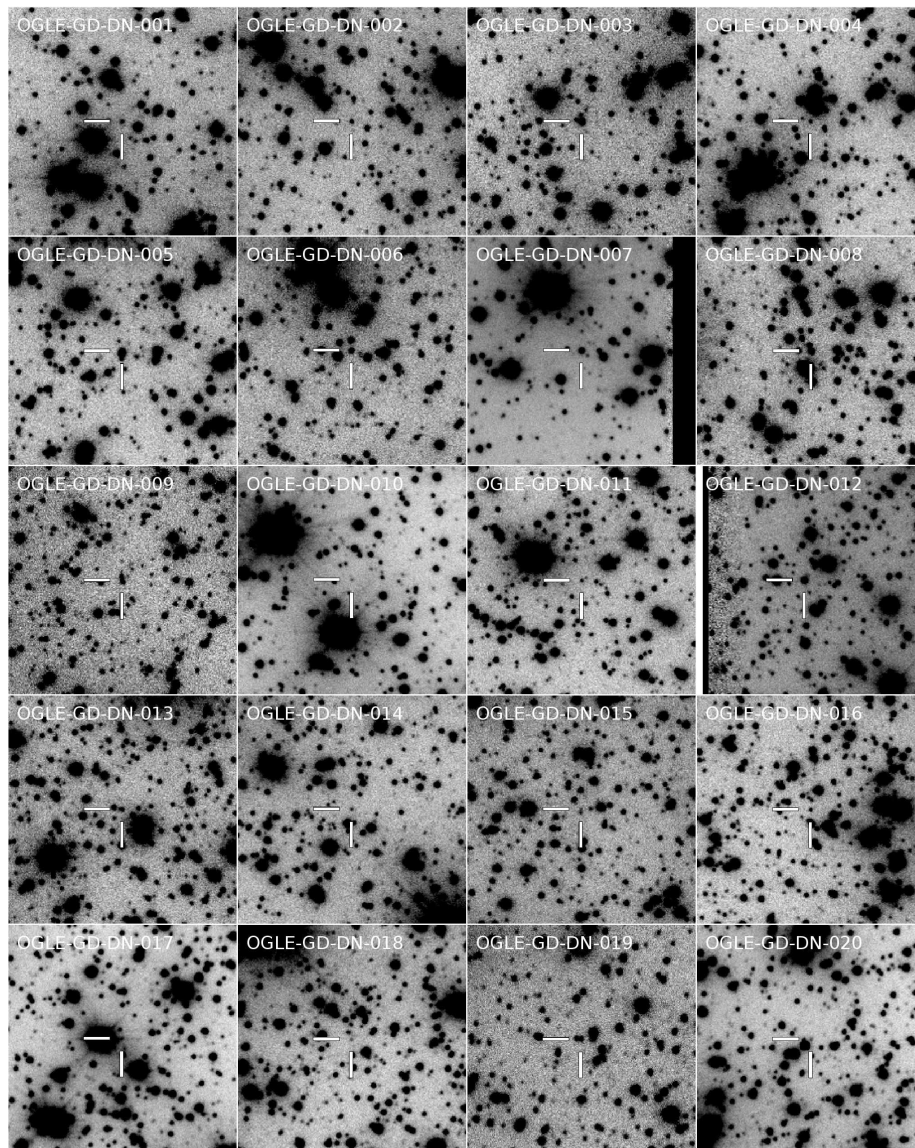


Fig. 2. Finding charts for the newly discovered DNe in the OGLE-III disk data (part 1 of 2). North is to the right and East is up. The field of view is $1'$ on a side. The variables are exactly in the centers of the charts and marked with cross-hairs.

5 U Gem type Stars

In Table 2 we give basic photometric information on our U Gem type stars: the mean I -band brightness in quiescence I_{qui} , the mean I -band maximum brightness in outbursts I_{out} , the number of observed outbursts, the duration of outbursts D_{out} , the recurrence time between the outbursts T_{out} , and the orbital period P_{orb} . Figs. 4–5 present the light curves of DNe classified as U Gem type variables. Phased light curves for three systems with orbital periods estimated in quiescence are shown in Fig. 6.

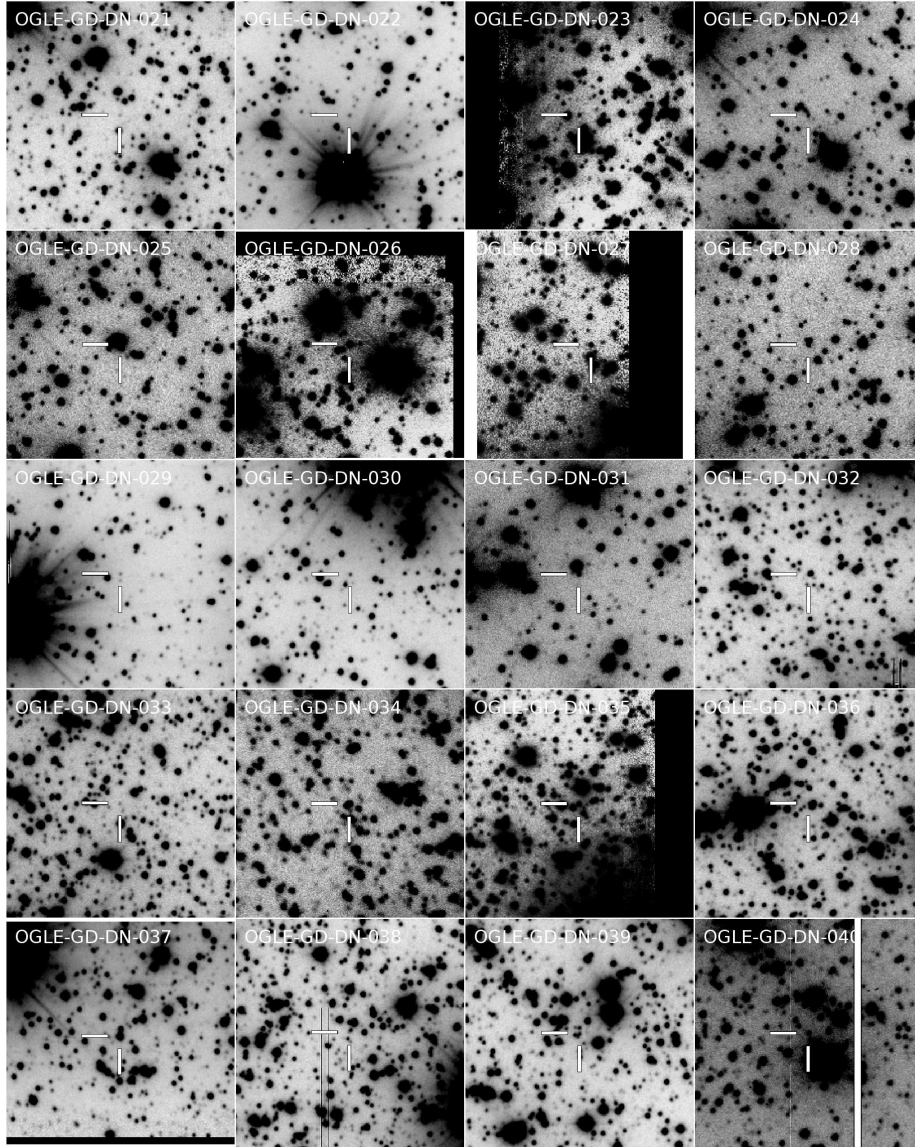


Fig. 3. Finding charts for the newly discovered DNe in the OGLE-III disk data (part 2 of 2). North is to the right and East is up. The field of view is $1'$ on a side. The variables are exactly in the centers of the charts and marked with cross-hairs.

5.1 OGLE-GD-DN-002

This star was observed during two seasons: 2007 and 2008. Its global light curve is shown in the most upper panel of Fig. 4. The scattered data points under the main light curve are real variations due to eclipses. In order to find the orbital period, we performed an $O - C$ analysis for two seasons separately. From the light curve we selected the data points corresponding to the primary minimum. We adopted a trial period of 0.178 d and calculated a linear ephemeris. The best period values are 0.177937(3) d and 0.177942(4) d for the 2007 and 2008 season, respectively. The estimated values do not differ statistically, therefore the derived orbital period is $P_{\text{orb}} = 0.177939(3) \text{ d} = 4.27053(6) \text{ h}$ and the upper limit for the period derivative is $\dot{P}_{\text{orb}} = +2 \cdot 10^{-8}$. The obtained orbital period

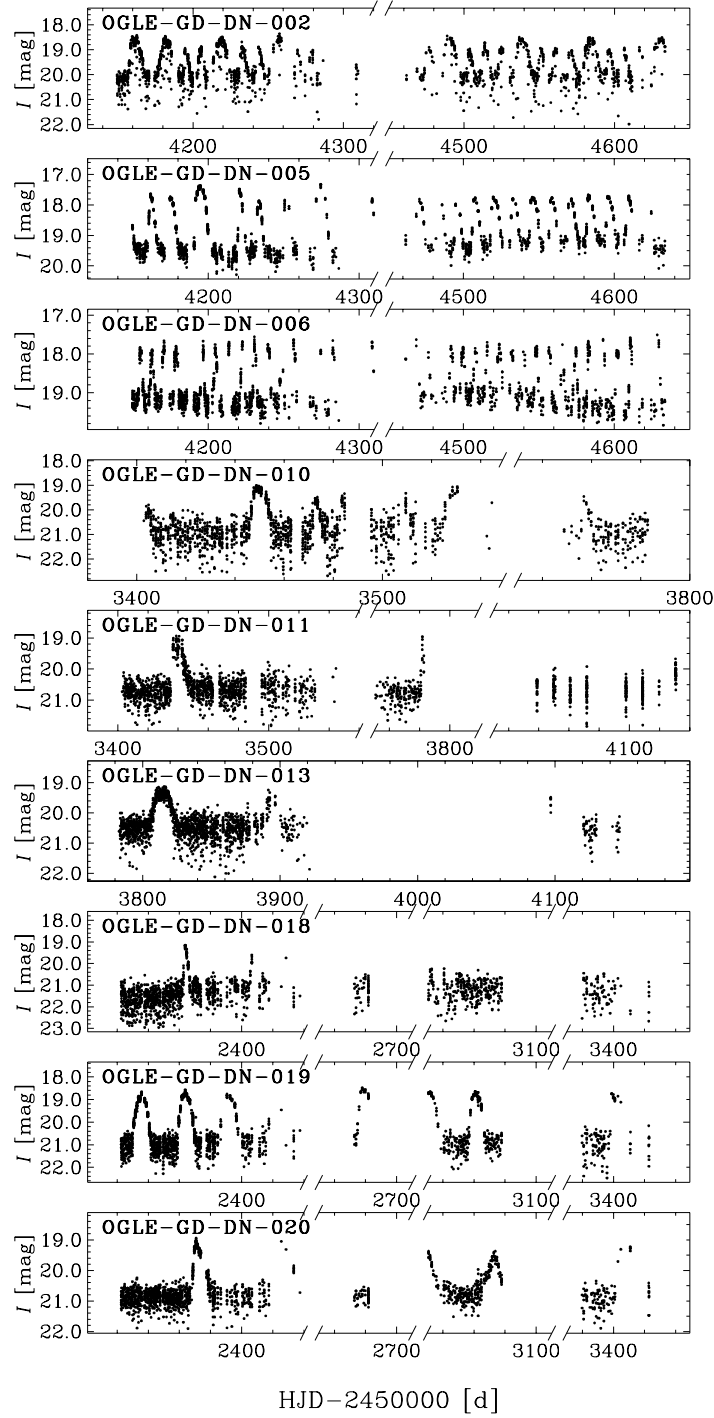


Fig. 4. Light curves of the U Gem type stars found in the OGLE-III disk area (part 1 of 2). Small ticks on the time axis are every 20 d.

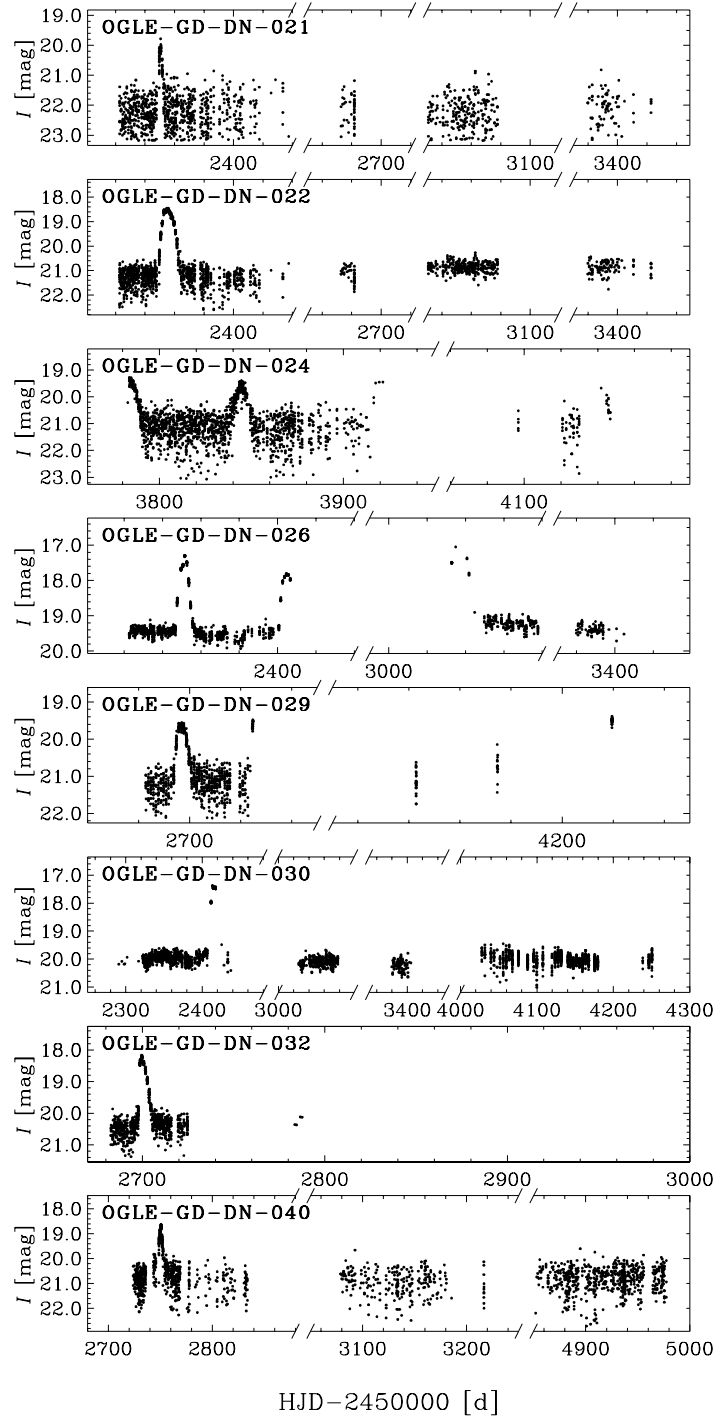


Fig. 5. Light curves of the U Gem type stars found in the OGLE-III disk area (part 2 of 2). Small ticks on the time axis are every 20 d. Objects with the measured brightness of $I \approx 22$ –23 mag in quiescence (e.g., OGLE-GD-DN-021) could be fainter in baseline.

Table 2: Photometric data on the detected U Gem type stars

Name	I_{qui} [mag]	I_{out} [mag]	n_{out}	D_{out} [d]	T_{out} [d]	P_{orb} [d]
OGLE-GD-DN-002	20.18	18.46	22	10.0	10.7	0.177939(3)
OGLE-GD-DN-005	19.56	17.71	22	6.6	12.6	-
OGLE-GD-DN-006	19.23	17.74	33	3.0	8.6	0.269963(9)
OGLE-GD-DN-010	20.99	19.03	7	9.0	11.5	-
OGLE-GD-DN-011	20.70	18.95	3	11.0	-	-
OGLE-GD-DN-013	20.51	19.13	3	21.0	81.0	-
OGLE-GD-DN-018	21.21	18.95	3	5.0	-	-
OGLE-GD-DN-019	21.02	18.63	7	12.1	29.0	0.426916(3)
OGLE-GD-DN-020	20.87	18.95	5	13.0	54.5	0.293191(3)
OGLE-GD-DN-021	22.19	19.78	1	4.0	-	-
OGLE-GD-DN-022	21.23	18.45	1	15.5	-	-
OGLE-GD-DN-024	21.12	19.34	4	13.0	61.0	-
OGLE-GD-DN-026	19.38	17.34	3	10.0	52.8	-
OGLE-GD-DN-029	21.19	19.47	3	8.0	27.2	-
OGLE-GD-DN-030	19.99	17.38	1	> 8.0	-	-
OGLE-GD-DN-032	20.35	18.16	1	8.0	-	-
OGLE-GD-DN-040	20.70	18.63	1	6.0	-	-

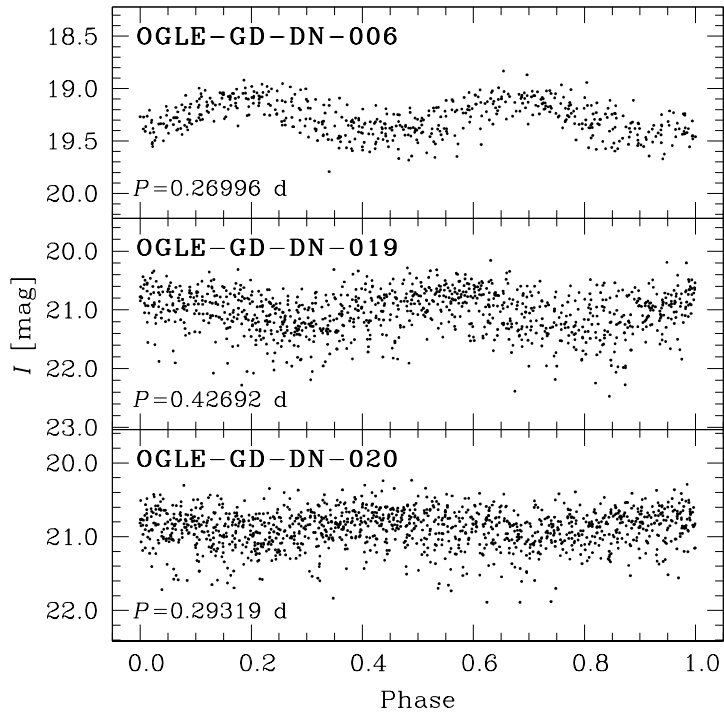


Fig. 6. Phased light curves of three U Gem type stars in quiescence.

places OGLE-GD-DN-002 well above the period gap, in contrast to what one would expect from its global light curve at the first glance. With the bright (long) and faint (short) outbursts it might resemble an SU-UMa type variable, but it is not.

We detrended and phased the light curve during the short outbursts, long outbursts, and in quiescence (see Fig. 7). During outbursts the primary eclipses are deeper (≈ 1.8 mag) than in quiescence (≈ 1.0 mag), which can be easily explained: during outbursts the temperature of the accretion disk rises. Simultaneously, in that phase, the depth of the secondary eclipse decreases. During bright and long outbursts, the secondary eclipses are practically not visible.

We also report the presence of an embedded precursor in one of the long outbursts in OGLE-GD-DN-002 (see Fig. 8). Embedded precursors have been found in V447 Lyr based on the Kepler data (Ramsay *et al.* 2012) and in archival data of U Gem and SS Cyg (Cannizzo 2012). Studies of such features may help in understanding of the mechanism of long outbursts in DNe in general.

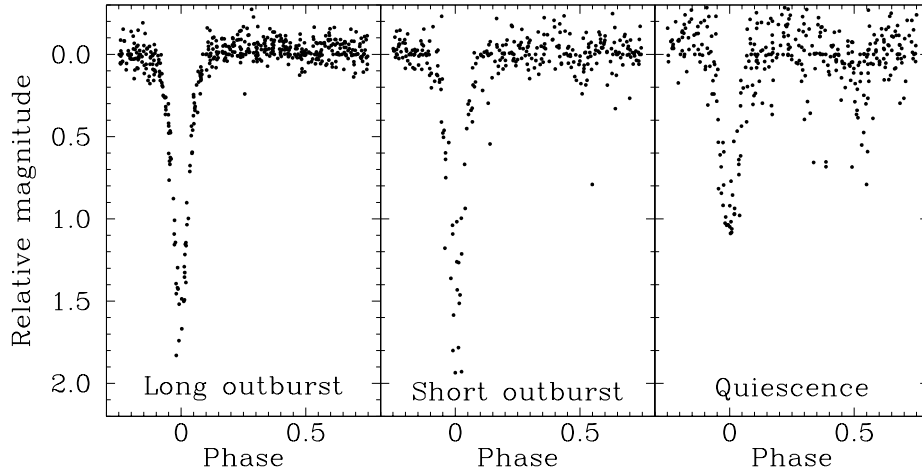


Fig. 7. Eclipses in OGLE-GD-DN-002 in three different states.

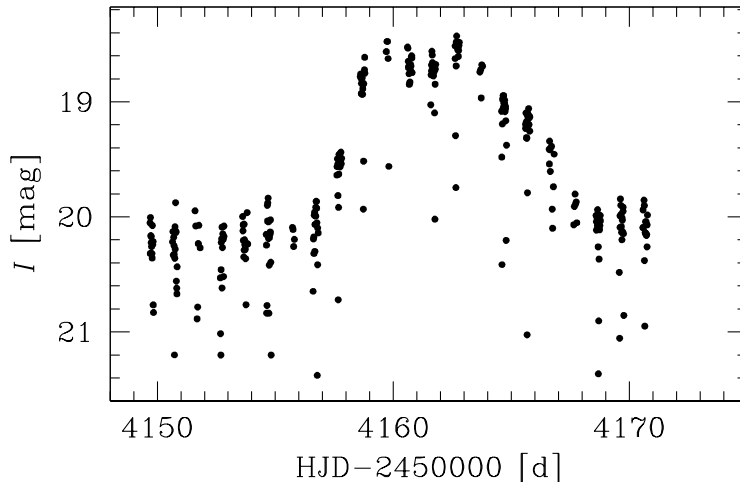


Fig. 8. Close-up on the outburst with an embedded precursor in OGLE-GD-DN-002.

Table 3: Photometric data on the SU UMa- and WZ Sge type variables

Name	I_{qui} [mag]	I_{n} [mag]	I_{s} [mag]	n_{n}	n_{s}	D_{n} [d]	D_{s} [d]	T_{n} [d]	T_{s} [d]	P_{sh} [d]
OGLE-GD-DN-001	21.63	19.24	17.80	4	1	2.0	18.0	-	-	0.06072(2)
OGLE-GD-DN-003	20.19	17.88	17.50	16	6	6.5	11.6	11.7	55.0	-
OGLE-GD-DN-004	21.00	18.72	18.38	25	11	4.5	7.1	6.9	24.5	-
OGLE-GD-DN-007	18.01	17.33	17.17	1	2	3.0	12.0	-	-	0.08081(4)
OGLE-GD-DN-008	22.05	18.16	17.82	2	1	4.5	18.0	-	-	0.08404(3)
OGLE-GD-DN-009	19.73	17.36	16.96	21	4	6.0	11.0	14.5	86.8	0.1310(3)
OGLE-GD-DN-014	22.65	19.68	> 18.44	2	1	3.5	> 8.0	-	-	0.08931(5)
OGLE-GD-DN-015	20.65	18.74	18.27	3	1	5.5	11.0	-	-	-
OGLE-GD-DN-016	20.54	-	18.21	0	1	-	18.0	-	-	-
OGLE-GD-DN-017	21.57	18.61	> 18.47	1	1	4.0	> 9.0	-	-	-
OGLE-GD-DN-023	22.17	20.89	19.90	2	3	-	13.0	-	-	-
OGLE-GD-DN-025	18.39	-	17.28	0	1	-	18.0	-	-	-
OGLE-GD-DN-031	20.34	18.99	18.34	3	2	3.0	12.0	-	-	0.06324(1)
OGLE-GD-DN-033	22.08	19.69	19.32	6	3	4.6	10.0	18.0	-	-
OGLE-GD-DN-034	20.98	18.50	17.43	5	2	5.0	> 14.0	-	-	-
OGLE-GD-DN-036	21.91	20.08	19.69	13	8	4.4	10.3	11.4	55.3	-
OGLE-GD-DN-037	16.19	-	15.88	0	3	-	14.8	-	-	-
OGLE-GD-DN-038	20.76	-	19.19	0	1	-	14.0	-	-	-
OGLE-GD-DN-039	19.76	18.63	18.20	35	5	2.7	13.0	4.5	80.0	0.08349(7)

6 SU UMa- and WZ Sge type Stars

In Table 3, we list basic photometric properties of stars identified as SU UMa- and WZ Sge type variables: the mean brightness in quiescence I_{qui} , the mean maximum brightness in normal outburst I_{n} and in superoutburst I_{s} , the number of observed normal outbursts n_{n} and superoutbursts n_{s} , the duration of normal outbursts D_{n} and superoutbursts D_{s} , the recurrence time between the normal outbursts T_{n} , the supercycle length T_{s} , and the superhump period P_{sh} , if measured. Light curves of SU UMa type variables, except for the WZ Sge type stars OGLE-GD-DN-001 and OGLE-GD-DN-014, are shown in Figs. 9–10. Below we describe selected objects in detail.

6.1 OGLE-GD-DN-003

A typical supercycle in this star lasts 55 d and contains three normal outbursts. One of the supercycles, the one around HJD=2454200, is shorter: 52 d with two normal outbursts. During that supercycle normal outbursts lasted longer (15.8 ± 0.1 d) in comparison to outbursts during the other supercycles (11.7 ± 0.2 d). Distinct precursor outbursts were observed prior to superoutbursts. In quiescence, a periodic signal with $0.15162(1)$ d was found.

6.2 OGLE-GD-DN-004

This star has the shortest measured supercycle length in our sample of SU UMa type DNe. We found that the supercycle increased from 24.5 ± 0.1 d in 2007 to 26.4 ± 0.1 d in 2008. This corresponds to $\dot{P}_{\text{sc}} = (+5.4 \pm 0.6) \cdot 10^{-3}$. During the 2007 season the supercycles were very similar to each other, while in 2008 the outbursts seemed to be more erratic. We note the presence of precursors before some superoutbursts.

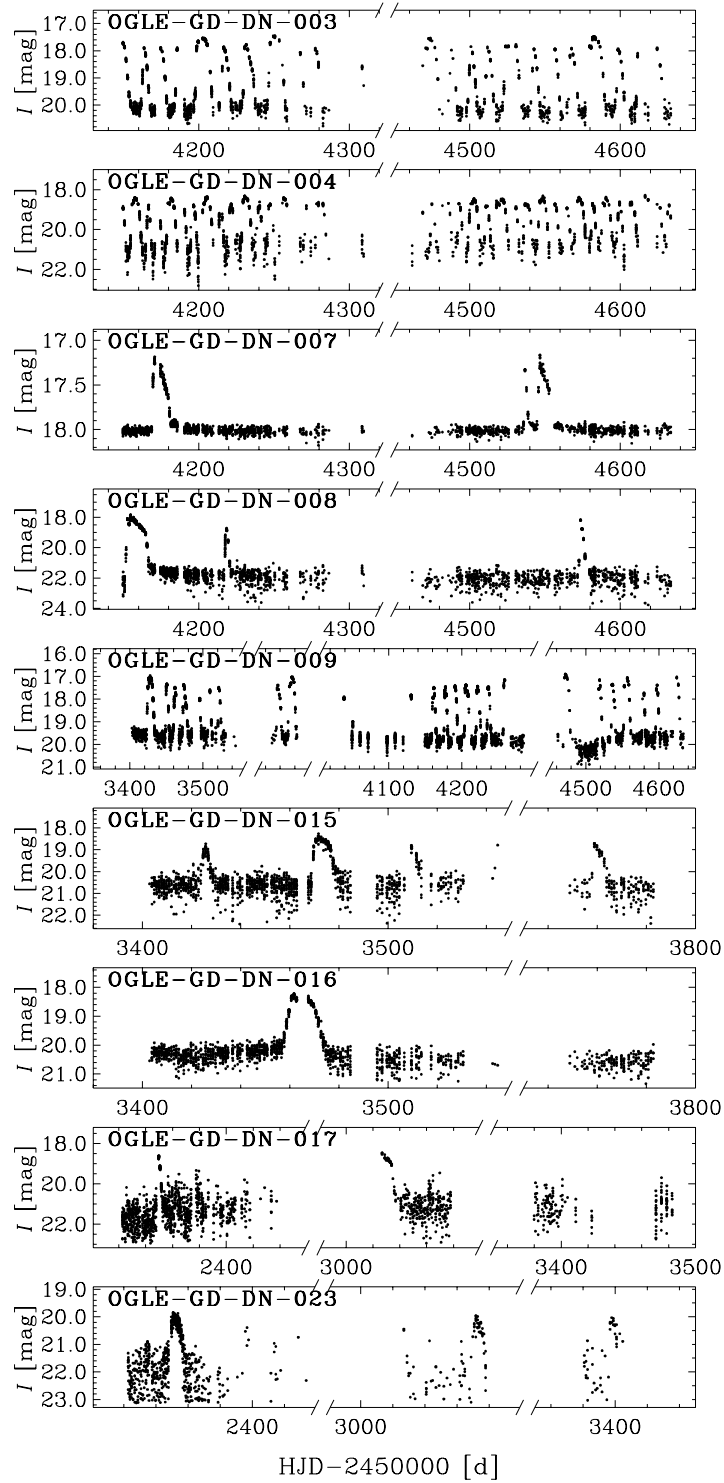


Fig. 9. Light curves of the SU UMa type stars detected in the OGLE-III disk fields (part 1 of 2). Small ticks on the time axis are every 20 d.

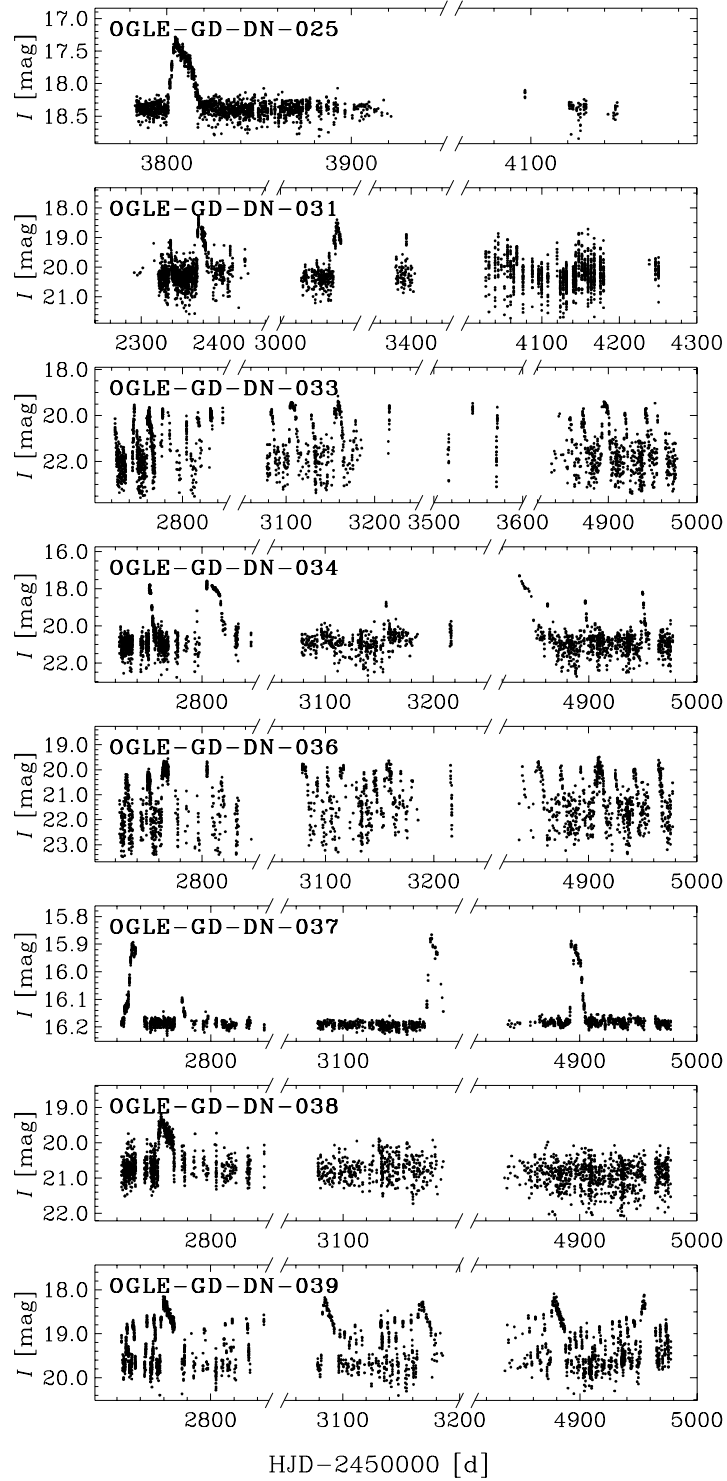


Fig. 10. Light curves of the SU UMa type stars detected in the OGLE-III disk fields (part 2 of 2). Small ticks on the time axis are every 20 d.

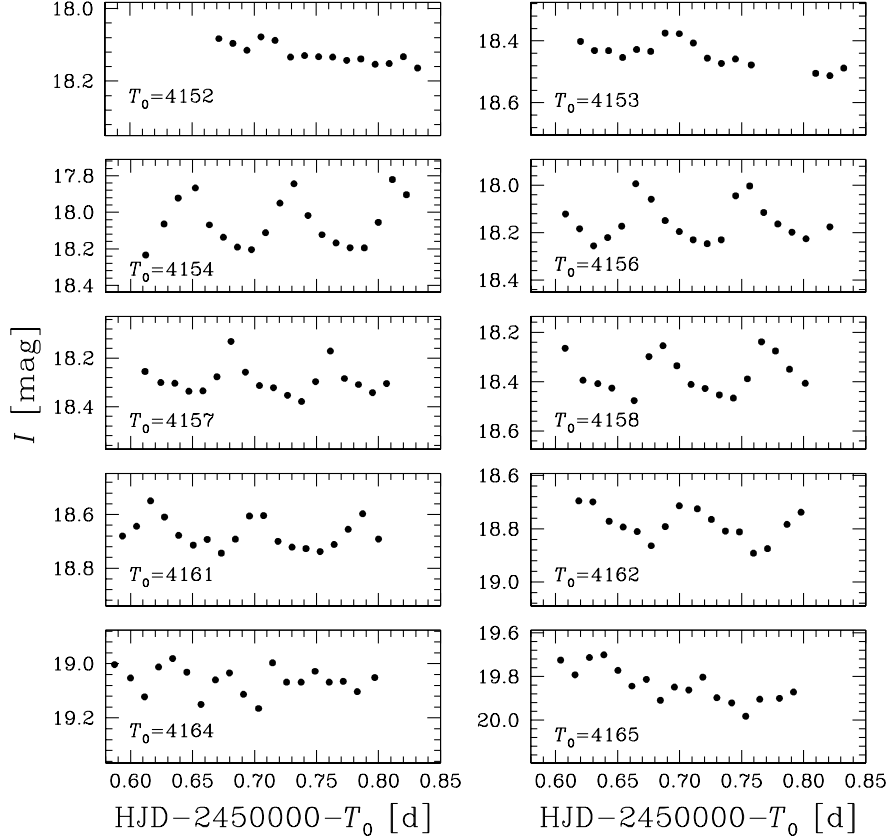


Fig. 11. Evolution of superhumps in the SU UMa type dwarf nova OGLE-GD-DN-008 during the superoutburst in 2007.

6.3 OGLE-GD-DN-007

In this star only two superoutbursts were observed with distinct superhumps with the period of 0.08081(4) d. Possible lengths of the supercycle are the following: 94 d, 125 d, 188 d or 376 d.

6.4 OGLE-GD-DN-008

In the light curve of this SU UMa type variable only one superoutburst was noted. The lower limit for the supercycle length is about 160 d. Superhumps, already observed during the precursor outburst, have the period of 0.08404(3) d. The superhump evolution is shown in Fig. 11.

6.5 OGLE-GD-DN-009

This star is located in two overlapping OGLE-III fields, CAR109 and CAR115, and was monitored for a record number of 379 nights over seasons 2005–2008. Four long and bright superoutbursts with distinct precursors and superhumps were observed. The estimated supercycle period amounts to 86.8 d, while the recurrence time of the normal outbursts increased systematically from 12 d to 19 d. The superhump period is 0.1310(3) d.

6.6 OGLE-GD-DN-023

This star is one of the faintest stars in our sample. Three bright superoutbursts and two normal outbursts were observed. The possible supercycle length is either 65.5 d or 80 d. During the first superoutburst we found low-amplitude variations (probably superhumps) with the period of either 0.0705(5) d or 0.0755(5) d.

6.7 OGLE-GD-DN-034

Only two superoutbursts were observed for this object. During the first one, superhumps with the period of 0.06324(1) d were found. The shortest plausible supercycle length for this star is 70 d, however other values are also possible.

6.8 OGLE-GD-DN-036

The supercycle length in this object increased from 43.7 ± 0.3 d in 2003 to 55.3 ± 0.7 d in 2004. This corresponds to $\dot{P}_{sc} = (+5.9 \pm 0.4) \cdot 10^{-3}$. The recurrence time between the normal outbursts varies significantly, from 7 d to 18 d with a mean value of 10–11 d.

6.9 OGLE-GD-DN-039

The light curve of this stars shows five bright ($I_{max} \approx 18.2$ mag) and long (≈ 13 d) superoutbursts and 10 normal outbursts in between ($I_{max} \approx 18.6$ mag, 2.7 ± 0.2 d). Although no precursor outbursts were observed (unluckily, due to bad weather conditions the beginning of two superoutbursts were missed), the presence of superhumps indicates that this object is a *bona fide* SU UMa type variable. The superhump period amounts to $P_{sh} = 0.08349(7)$ d = 2.004(2) h. The average supercycle length is 80.0(1) d, however, it decreased from 81.5 d to 78.4 d with a constant rate of $\dot{P}_{sc} = -1.36(8) \cdot 10^{-3}$. This is in contradiction to what has been recently found in active SU UMa type stars (Otulakowska-Hypka *et al.* 2013b). The object OGLE-GD-DN-039 seems to be one of the missing systems between the typical SU UMa type variables and ER UMa type stars.

6.10 OGLE-GD-DN-001 and OGLE-GD-DN-014

These two WZ Sge type stars have similar light curves, shown in Fig. 12. In both cases we observed bright and long superoutburst with distinct superhumps followed by a series of 2–4 short “echo” outbursts. The *I*-band amplitude of the superoutbursts are 2.9 mag and 4.2 mag in OGLE-GD-DN-001 and OGLE-GD-DN-014, respectively, while the “echo” outbursts are ≈ 1.4 mag fainter, in both stars. Unfortunately, the beginnings of the superoutbursts were not observed. In OGLE-GD-DN-001 the points around HJD=2454170 may correspond to the precursor outburst. We assessed the superhump period for each star. For OGLE-GD-DN-001 it is equal to 0.06072(2) d = 1.4572(3) h. The second star, OGLE-GD-DN-014, has a slightly longer superhump period, P_{sh} , of 0.08931(5) d = 2.1434(10) h.

These two stars are very similar in their behavior to EG Cnc which was observed in superoutburst in 1996 (Patterson *et al.* 1998). This suggests that OGLE-GD-DN-001 and OGLE-GD-DN-014 are WZ Sge type stars with a very small mass-transfer rate and extremely long supercycles. Two similar systems, namely MBR124.21.11N and MBR120.21.138N, were recently discovered in the

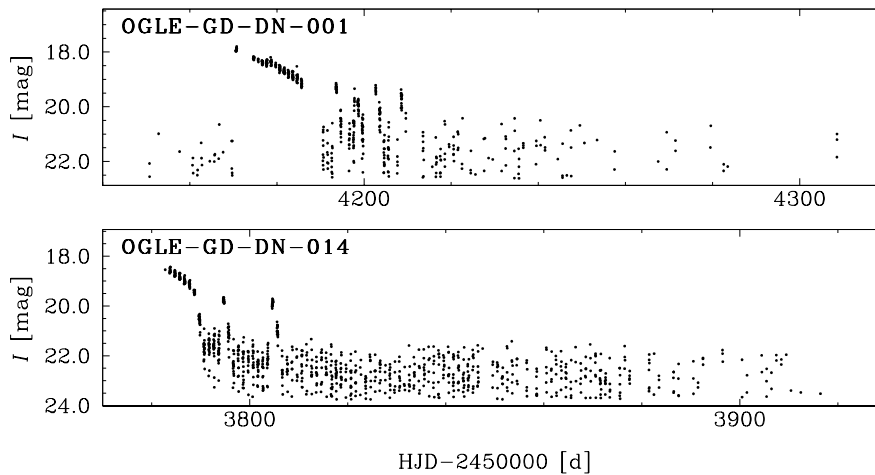


Fig. 12. Light curves of two WZ Sge type stars. Note the presence of “echo” outbursts after the superoutbursts.

Table 4: Photometric data on the newly discovered Z Cam type stars

Name	I_{stand} [mag]	I_{max} [mag]	I_{min} [mag]	D_{out} [d]	T_{out} [d]
OGLE-GD-DN-012	17.71	17.13	18.28	6-8	9
OGLE-GD-DN-027	19.15	18.35	19.71	8-15	20
OGLE-GD-DN-028	19.70	18.37	20.15	6-16	26
OGLE-GD-DN-035	18.73	17.62	20.63	7-16	17-20

OGLE Magellanic Bridge region (Kozłowski *et al.* 2013). Future OGLE observations should allow estimation of the supercycle lengths in all these objects.

7 Z Cam type Stars

Basic photometric properties of four Z Cam type stars in the OGLE-III disk area are listed in Table 4. We measured the following values: the mean brightness in standstill I_{stand} , the maximum I_{max} and minimum I_{min} brightness in outburst, the duration of outbursts D_{out} , and the recurrence time between outbursts T_{out} . Light curves of the stars are plotted in Fig. 13. The detected Z Cam type stars spent on average 25% of the time in standstills. Below we give detail comments on each object.

7.1 OGLE-GD-DN-012

This star was observed for two seasons (2005–2006). In its light curve, one can see fainter ($I_{\text{max}} \approx 17.5$ mag, $\text{amp}_I \approx 0.6$ mag) and shorter (5–6 d) regular outbursts interlaced every 3–4 events with more prominent ($I_{\text{max}} \approx 17.1$ mag, $\text{amp}_I \approx 1.1$ mag) and longer (10–11 d) outbursts. In minimum, the I -band brightness is 18.3 mag and is similar after both types of outbursts. It is worth to note that, in contrast to the majority of known Z Cam type stars, the brightness in OGLE-GD-DN-012 increased after the first standstill. Unfortunately, the end of the second standstill was not observed.

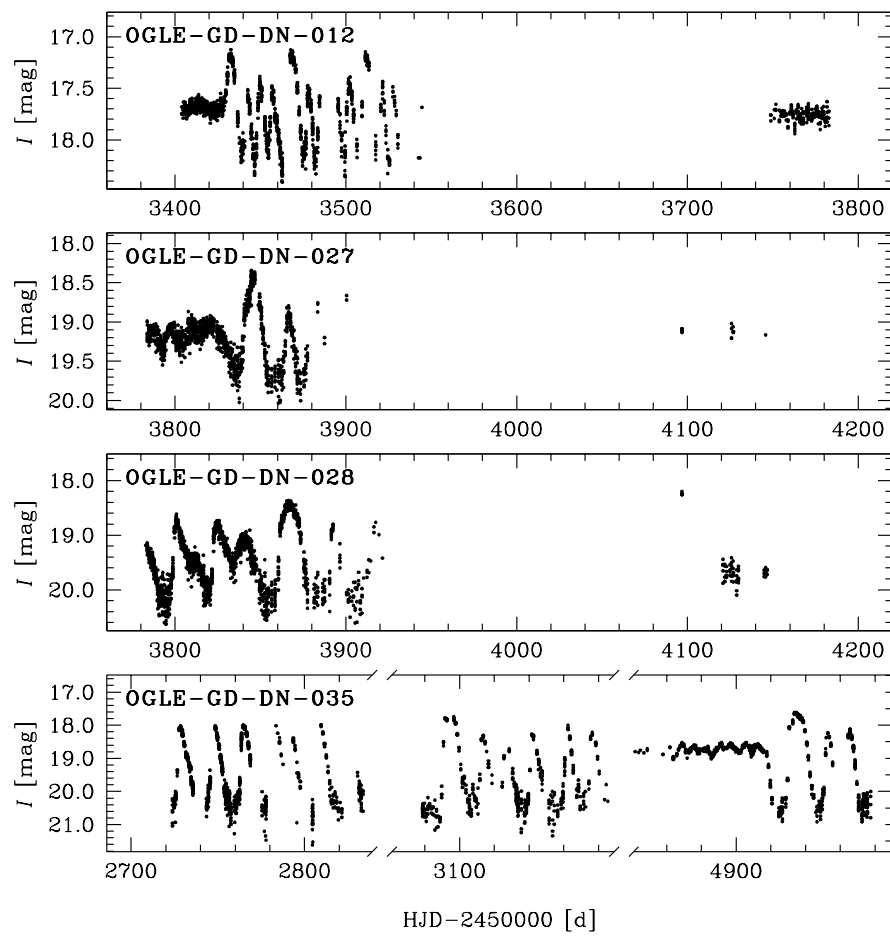


Fig. 13. Light curves of Z Cam type stars.

7.2 OGLE-GD-DN-027

We observed one clear standstill for this star. The first outburst after the standstill was brighter and longer ($I_{\max} \approx 18.35$ mag, 15 d) than the following three outbursts ($I_{\max} \approx 18.80$ mag, 8 d). During the standstill the brightness varied with an amplitude of ≈ 0.5 mag and a time scale of ≈ 12 d.

7.3 OGLE-GD-DN-028

In this object two very short standstills were observed, around HJD=2453810 and HJD=2454120. The I -band amplitudes of 1.2–2.0 mag and irregular shape of the outbursts are typical for Z Cam type stars.

7.4 OGLE-GD-DN-035

This is the best observed Z Cam type star in our sample. Its light curve covers 279 nights over years 2003–2009. It includes 15 outbursts and one standstill lasting at least 60 d. In the first two seasons, the star exhibited outbursts recurring every 17–20 d. The first outburst after the standstill was brighter and longer ($I_{\max} \approx 17.6$ mag, 16 d) than the following ones ($I_{\max} \approx 18.1$ mag, 7 d). OGLE-GD-DN-035 was observed in the standstill phase for about 22% of the time. In this state the brightness variations with an amplitude of ≈ 0.4 mag and a time scale of ≈ 7.5 d were seen.

8 Summary and Conclusions

In this paper we report the identification of forty new dwarf novae in twenty-one OGLE-III Galactic disk fields. We have increased the total number of all known DNe by 7 per cent. Seventeen variables are of the U Gem type, nineteen of the SU UMa type, and four of the Z Cam type. We analyzed the light curves and estimated basic parameters of the DNe such as the duration and recurrence period of the outbursts. Prominent eclipses seen in OGLE-GD-DN-002 allowed us to find precise orbital period in this system. We note that in one of our Z Cam type objects, OGLE-GD-DN-012, in contrast to the large majority of variables of this type, we observed an increase of brightness after the standstill phase.

In the case of five DNe classified as SU UMa type variables we were able to assess supercycle lengths. The obtained lengths are in the range 20–90 d, generally between objects classified as typical SU UMa type and ER UMa type variables. In Fig. 14, we present the distribution of the supercycle lengths for 73 known SU UMa type stars, including the five new objects. The number of detected short supercycle period DNe is large enough to discard the ER UMa type as a separate class of variables and to classify them as SU UMa type variables. We note that in object OGLE-GD-DN-039 we found a decrease in the supercycle period — not observed in other active SU UMa type systems.

Currently, there is no known DN with a supercycle period between 1100 d and 3300 d. Dozens of systems with a single observed WZ Sge-like superoutburst require follow-up monitoring campaigns with the aim to find their P_{sc} . In this paper we add two stars, OGLE-GD-DN-001 and OGLE-GD-DN-014, to the list of such systems. Analysis of time-series photometry from existing (*e.g.*, 21-year-long bulge observations by OGLE) and future long-term surveys (*e.g.*, Large Synoptic Survey Telescope, LSST Science Collaboration 2009)

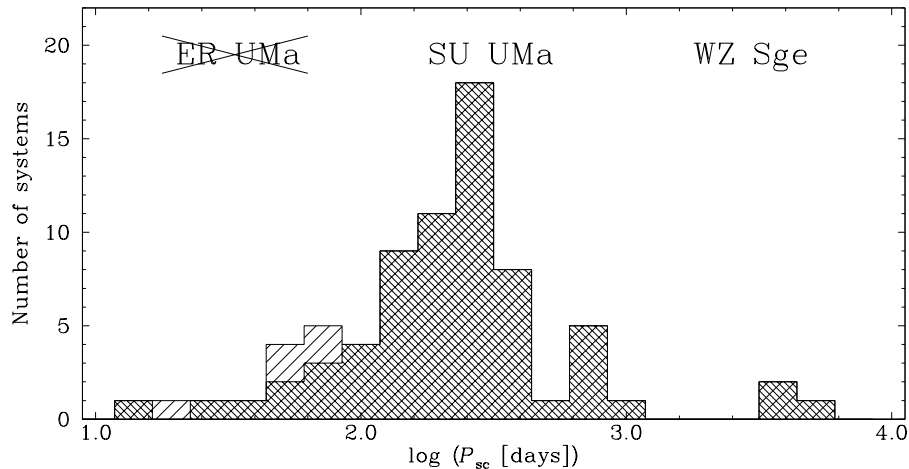


Fig. 14. Distribution of the supercycle lengths for known SU UMa type stars. Five OGLE stars have, more or less, supercycle lengths between the short period ER UMa type stars and the typical SU UMa type DNe. Thus, we propose to discard the former type.

should allow statistical assessment of the existence of objects with P_{sc} in this range.

Acknowledgments. This work has been supported by the Polish National Science Centre grant No. DEC-2011/03/B/ST9/02573 and the Polish Ministry of Sciences and Higher Education grant No. IP2012 005672 under Iuventus Plus programme.

The OGLE project has received funding from the European Research Council under the European Community's Seventh Framework Programme (FP7/2007-2013)/ERC grant agreement No. 246678 to A.U.

REFERENCES

- Alard, C., and Lupton, R. H. 1998, *Astrophys. J.*, **503**, 325.
 Balman, S. 2012, *Memorie della Societa Astronomica Italiana*, **83**, 585.
 Boyle, B. J., et al. 2000, *MNRAS*, **317**, 1014.
 Cannizzo, J. K., Still, M. D., Howell, S. B., Wood, M. A., and Smale, A. P. 2010, *Astrophys. J.*, **725**, 1393.
 Cannizzo, J. K. 2012, *Astrophys. J.*, **757**, 174.
 Cannizzo, J. K., Smale, A. P., Wood, M. A., Still, M. D., and Howell, S. B. 2012, *Astrophys. J.*, **747**, 117.
 Cieslinski, D., Diaz, M., Mennickent, R., and Pietrzyński, G. 2003, *P.A.S.P.*, **115**, 193.
 Cieslinski, D., Diaz, M., Drake, A., and Cook, K. 2004, *P.A.S.P.*, **116**, 610.
 Drake, A. J., Djorgovski, S. G., Mahabal, A., Prieto, J. L., Beshore, E., Graham, M. J., Catalan, M., Larson, S., Christensen, E., Donalek, C., and Williams, R. 2012, *Proceedings of the International Astronomical Union, IAU Symposium*, **285**, 306.
 Gänsicke, B. 2005, *Proceedings of ASP Conference*, **330**, 3.
 Green R. F., Schmidt M., Liebert J. 1986, *Astrophys. J. Suppl. Ser.*, **61**, 305.
 Hagen, H.J., Grootte, D., Engels, D., and Reimers, D. 1995, *Astron. Astrophys. Suppl. Ser.*, **111**, 195.
 Koch, D. G. et al. 2010, *Astrophys. J.*, **713**, L79.
 Kozłowski, S., Udalski, A., Wyrzykowski, L., Poleski, R., Pietrukowicz, P., Skowron, J., Szymański, M. K., Kubiak, M., Pietrzyński, G., Soszyński, I., and Ulaczyk, K. 2013, *Acta Astron.*, **63**, 1.
 Law, N. M., et al. 2009, *P.A.S.P.*, **121**, 1395.
 LSST Science Collaboration 2009, *LSST Science Book, Version 2.0*, arXiv0912.0201.
 Meyer, F., and Meyer-Hofmeister, E. 1983, *Astron. Astrophys.*, **121**, 29.

- Osaki, Y. 1974, *PASJ*, **26**, 429.
- Osaki, Y. 1989, *PASJ*, **41**, 1005.
- Osaki, Y., and Kato, T. 2013, *PASJ*, **65**, 50.
- Otulakowska-Hypka, M., Olech, A., de Miguel, E., Rutkowski, A., Koff, R., and Bąkowska, K. 2013a, *MNRAS*, **429**, 868.
- Otulakowska-Hypka, M., and Olech, A. 2013b, *MNRAS*, **in print**, arXiv:1303.6248.
- Patterson, J., *et al.* 1998, *P.A.S.P.*, **110**, 1290.
- Payne-Gaposchkin, C., and Gaposchkin, S. 1938, “*Variable stars*”, **Cambridge, Mass.**, The observatory.
- Pietrukowicz, P., Mróz, P., Soszyński, I., Udalski, A., Poleski, R., Szymański, M. K., Kubiak, M., Pietrzyński, G., Wyrzykowski, L., Ulaczyk, K., Kozłowski, S., and Skowron, J. 2013, *Acta Astron.*, **63**, NNN.
- Pojmański, G. 1997, *Acta Astron.*, **47**, 467.
- Poleski, R., Udalski, A., Skowron, J., Szymański, M. K., Kubiak, M., Pietrzyński, G., Soszyński, I., Kozłowski, S., Pietrukowicz, P., Wyrzykowski, L., and Ulaczyk, K. 2011, *Acta Astron.*, **61**, 123.
- Ptak, A., and Griffiths, R. 2003, *ASPC*, **295**, 465.
- Ramsay, G., Cannizzo, J. K., Howell, S. B., Wood, M. A., Still, M., Barclay, T., and Smale, A. 2012, *MNRAS*, **425**, 1479.
- Ritter, H., and Kolb, U. 2003, *Astron. Astrophys.*, **404**, 301.
- Samus, N. N., *et al.* 2013, , , General Catalog of Variable Stars, Version: Apr 2013.
- Schwarzenberg-Czerny, A. 1996, *Astrophys. J.*, **460**, L107.
- Smak, J. I. 1991, *Acta Astron.*, **41**, 269.
- Smak, J. 2004, *Acta Astron.*, **54**, 221.
- Smak, J. 2008, *Acta Astron.*, **58**, 55.
- Stobie R. S. 1997, *MNRAS*, **287**, 848.
- Szkody, P., *et al.* 2011, *Astron. J.*, **142**, 181.
- Szymański, M. K., Udalski, A., Soszyński, I., Kubiak, M., Pietrzyński, G., Poleski, R., Wyrzykowski, L., and Ulaczyk, K. 2010, *Acta Astron.*, **60**, 295.
- Udalski, A. 2003, *Acta Astron.*, **53**, 291.
- Udalski, A., Szymański, M. K., Soszyński, I., and Poleski, R. 2008, *Acta Astron.*, **58**, 69.
- Udalski, A., Kowalczyk, K., Soszyński, I., Poleski, R., Szymański, M.K., Kubiak, M., Pietrzyński, G., Kozłowski, S., Pietrukowicz, P., Ulaczyk, K., Skowron, J., and Wyrzykowski, L. 2012, *Acta Astron.*, **62**, 133.
- Uemura, M., Kato, T., Nogami, D., and Ohsugi, T. 2010, *PASJ*, **62**, 613.
- Warner, B. 1995, *Camb. Astrophys. Ser.*, **28**, “Cataclysmic Variable Stars”, Cambridge University Press.
- Woźniak, P. R. 2000, *Acta Astron.*, **50**, 421.
- York, D. G. 2000, *Astron. J.*, **120**, 1579.